Journal of Molecular Catalysis A: Chemical 338 (2011) 18–23

Contents lists available at ScienceDirect

Journal of Molecular Catalysis A: Chemical

journal homepage: www.elsevier.com/locate/molcata

Band gap and photocatalytic properties of Ti-substituted hydroxyapatite: Comparison with anatase-TiO_2

Mineharu Tsukada[a,*], Masato Wakamura[a], Naoya Yoshida[b], Toshiya Watanabe[b]

[a] Device and Materials Laboratories, Fujitsu Laboratories Ltd., 10-1 Morinosato-Wakamiya, Atsugi, Kanagawa 243-0197, Japan
[b] Research Center for Advanced Science and Technology, The University of Tokyo, 4-6-1 Komaba, Meguro-ku, Tokyo 153-8904, Japan

ARTICLE INFO

Article history:
Received 2 September 2010
Received in revised form
23 December 2010
Accepted 17 January 2011
Available online 27 January 2011

Keywords:
Photocatalysis
Band gap
First principles
Titanium substitution
Hydroxyapatite

ABSTRACT

We experimentally and theoretically evaluated the effect of Ti substitution in hydroxyapatite (HAP) on the band gap. For samples, we used 10 mol% of Ti-substituted HAP (Ti-HAP) and normal HAP powder, synthesized by the co-precipitation method, with typical anatase-TiO_2 photocatalytic powder. The Ti-HAP and HAP powder showed a hexagonal apatite structure by X-ray diffraction. The experimentally obtained optical band gap energies of Ti-HAP, HAP and TiO_2 powder measured by diffuse reflectance spectroscopy were 3.65 eV, >6 eV, and 3.27 eV, respectively. Depending on total energy evaluation and structure optimization by the first principle density functional calculation, the Ti position in the apatite structure was predicted to be at columnar, Ca(I), site with a Ca(I) site deficiency. In Ti-HAP, Ti 3d orbital hybridized with O 2p orbital and formed an internal state in the HAP band gap. It caused absorption-edge lowering of Ti-HAP. Based on the band structure, we proposed a photocatalytic model of Ti-HAP as a two-step excitation model. Moreover, acetaldehyde gas decomposition of Ti-HAP by UV with VIS irradiation appeared to be enhanced compared with when UV irradiation alone was used. We confirmed the validity of the proposed model.

1. Introduction

Hydroxyapatite (HAP) is one of the primary constituents of the biological hard tissues, and has been of interest in the industrial, medical and dental fields. Synthetic HAP finds many applications as an adsorbent for chromatography to separate protein and enzymes, a catalyst for dehydration and dehydrogenetion of alcohols, methane oxidation, and artificial teeth and bones [1–6]. Perfect HAP crystal is a monoclinic-type compound. However, typical HAP, which has a lattice deficiency, is a hexagonal-type ionic compound that has the $P6_3/m$ space group, with 44 atoms per unit cell. The chemical formula of HAP is $Ca_{10}(PO_4)_6(OH)_2$. The Ca ions are separated into two inequivalent sites, one is a columnar site along the *c* axis [hereafter, "Ca(I)"], and the other is located around OH [hereafter, "Ca(II)"] [1]. Since HAP has a complicated structure, many kinds of cations can be induced into the apatite crystal structure. Therefore, substituting cations in HAP can be done easily. Up to now, numerous cations were examined to substitute Ca ions in HAP [7–9]. On the other hand, Wakamura et al. prepared Ti-substituted hydroxyapatite (Ti-HAP), in which the Ca ions had been substituted by 10 mol% of Ti ions, and reported that Ti-HAP showed photocatalytic activity for near ultraviolet (UV) light, similar to anatase-TiO_2 [10]. As for the photocatalytic properties of HAP, Nishikawa et al. have reported the generation of $^{\bullet}OH$ and $O_2^{\bullet-}$ radicals on HAP after heat treatment at 200 °C and UV irradiation, and indicated the photocatalytic decomposition of methyl mercaptane and dimethyl disulfide under UV irradiation [11–16]. However, they were using a deep UV (254 nm) light source for the irradiation. Such phenomena require higher photon energy than does Ti-HAP. Therefore, the photocatalytic activity of Ti-HAP seems to be a new phenomenon caused by Ti substitution of HAP.

After the paper by Wakamura et al., several papers were published concerning Ti substitution in HAP and the photocatalytic activity of Ti-HAP [17–20]. However, precise structural analysis has not been performed for Ti-HAP, so that the location of the Ti ion in the apatite structure is not yet clear. Moreover, band gap evaluation of Ti-HAP, which is very important for understanding its photocatalytic properties, has not been done yet either. Few studies have been conducted to evaluate the band gap of apatite materials including HAP. In one paper, the band gap of HAP was reported to be 3.95 eV by photoluminessence measurement [21]. Recently, the number of studies related to the electronic structures of HAP by first principles calculations using the density functional theory (DFT) has been gradually increasing [22–32]. In some of these papers, the band gap of HAP was calculated and reported to be around 4.51–5.4 eV [23–25]. However, these values are larger than the

* Corresponding author. Tel.: +81 46 250 8166; fax: +81 46 250 8235.
E-mail address: mtsukada@labs.fujitsu.com (M. Tsukada).

1381-1169/$ – see front matter © 2011 Elsevier B.V. All rights reserved.
doi:10.1016/j.molcata.2011.01.017

experimental value of the band gap which was reported in Ref. [21]. In general, it is well known that a DFT calculation underestimates the value of the band gap compared with the true band gap. Therefore, it is impossible to interpret the band gap related electronic structure of HAP by depending on the experimental and theoretical results that have been obtained up to now. Moreover, there have been no studies conducted, either theoretically and experimentally on Ti-HAP, which is the target of this study. As a result, the photocatalytic mechanism of Ti-HAP remains unclear.

In this study, we evaluated the band gap of Ti-HAP both experimentally and theoretically. At first, we confirmed the crystal structure of Ti-HAP to be a hexagonal structure, to determine the base model structure for the first-principles calculations. Next, we experimentally measured the band gap and calculated the electronic structure by using the first-principle density functional theory (DFT) method. Moreover, we proposed a photocatalytic model of Ti-HAP. Lastly, we experimentally evaluated the photocatalytic activity of Ti-HAP to confirm our photocatalytic model. In addition, we also evaluated HAP and anatase-TiO_2 in the same way to compare and understand the photocatalytic properties of Ti-HAP.

2. Experimental and computational procedure

2.1. Materials, crystal structure and band gap evaluation

We obtained the HAP and Ti-HAP powders from Taihei Chemical Industrial Co. Ti-HAP was prepared experimentally based on Ref. [10]. The anatase-TiO_2 powder (ST-21) we used is a product of Ishihara Sangyo Kaisha Ltd. Ti-HAP powder, in which 10 mol% of Ca was substituted by Ti, was synthesized using the typical co-precipitation method in the similar way of HAP. Both HAP and Ti-HAP were calcined at 650 °C in 1 h by the authors. The details of the Ti-HAP preparation are described in Ref. [10]. The particle size of all materials was less than 100 nm. The crystal structures of the prepared HAP and Ti-HAP powders were identified by the X-ray diffraction (XRD) method (RINT 1500, Rigaku) using Cu Kα radiation (60 kV, 200 mA). The band gap energy was evaluated with diffuse reflectance spectra using a UV–VIS spectrophotometer with an integrating sphere (UV-3101PC, Shimazu). The wavelength range was 200–2500 nm. The reflection spectra were measured and transformed into an absorption coefficient using the Kubelka–Munk function, and the value of the band gap was determined by extrapolation.

2.2. Structure model and computational method

The electronic structure of Ti-HAP, HAP and anatase-TiO_2 was evaluated using a first principles pseudopotential calculation via the DFT method by using the Advance/PHASE code [33]. The generalized gradient approximation functional of Perdew, Burke, and Ernzerhof was used to calculate the exchange-correlation energy [34]. The wave function was expanded in a plane wave basis set up to an energy cutoff of 500 eV. Integration over the Brillouin zone was performed using the Monkhorst-Pack method with a $2 \times 2 \times 3$ mesh. For geometrical optimization, all atoms were allowed to relax until their forces converged to less than 5×10^{-4} hartree/bohr (0.026 eV/Å). Furthermore, the total and projector density of states (DOS) was calculated using the tetrahedron method for integration over the Brillouin zone with a $4 \times 4 \times 6$ mesh. The lattice parameter and bond angle of HAP and Ti-HAP were defined as $a = b = 9.4172$ Å, $c = 6.8799$ Å, $\alpha = \beta = 90°$, and $\gamma = 120°$, respectively. In the case of anatase-TiO_2, the lattice parameter was defined as $a = b = 3.7845$ Å, $c = 9.5413$ Å, $\alpha = \beta = \gamma = 90°$, and the k point mesh was set to $8 \times 8 \times 4$. Other parameters for calculations were same as those of HAP and Ti-HAP.

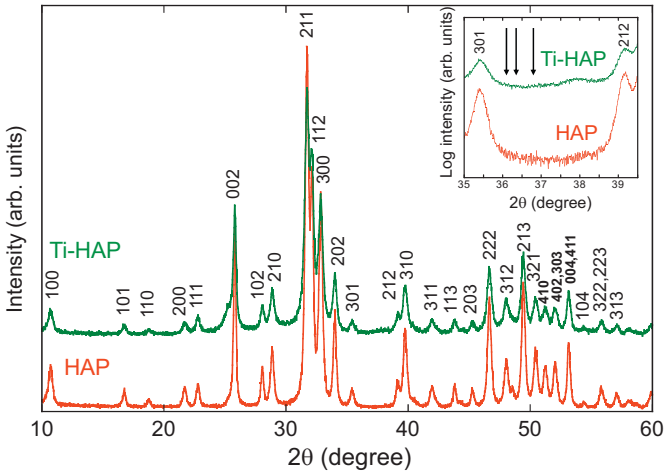

Fig. 1. XRD patterns of HAP and Ti-HAP powders. Inset shows enlarged diffraction patterns between 2θ of 35–39.5°. The arrows in the inset indicate the peak position of the monoclinic phase.

2.3. Photocatalytic activity for acetaldehyde gas decomposition

The photocatalytic activity was estimated from the decomposition of acetaldehyde vapor under UV, VIS and UV + VIS irradiation. The light source was Xe lamps (LA-251Xe, Hayashi Watch Works Co., Ltd.). The UV light (1.25 mW/cm^2) was obtained by cutting VIS with a color filter (UV-D36A, Asahi-Glass Co., Ltd.). VIS light (36,200 lux) was also obtained by cutting UV with a color filter (Y-43, Asahi-Glass Co., Ltd.). Moreover, UV + VIS light was made by mixturing the above-mentioned UV and VIS light. The sample weight was decided on by adjusting the surface area of the sample powders to a constant value of 85.5 m^2 using the BET (Brunauer–Emmett–Teller) method. The samples were allowed to settle at the bottom of a 500 cm^3 cylindrical glass vessel sealed with a quartz top plate with 5 mm thick, using an O-ring. A mixed gas (N_2, 80%; O_2, 20%) was introduced into the vessel through the gas inlet to replace the air with the mixed gas, and then acetaldehyde vapor was injected into the vessel to obtain 1% acetaldehyde concentration of initial atmosphere in the vessel. The vessels were kept in a dark environment until an adsorption equilibrium was achieved. Then, the sample powders were irradiated for 3 h. The concentration of CO_2 in the vessel was measured every 1 h with a gas chromatograph equipped with a flame ionization detector (GC 390B, GL Sciences).

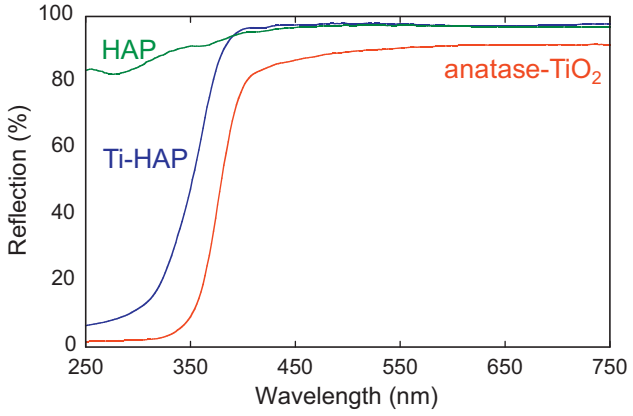

Fig. 2. Diffuse reflectance spectra of HAP, Ti-HAP and anatase-TiO_2 powders.

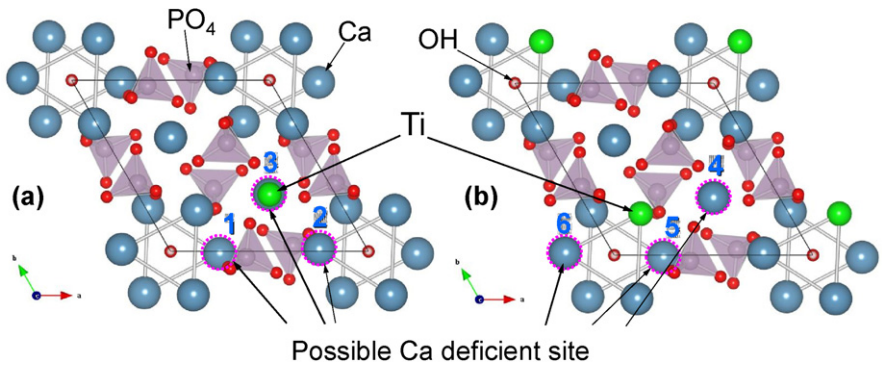

Fig. 3. Estimated Ti-HAP unit cell structures: (a) Ti-substituted Ca(I), (b) Ti-substituted Ca(II) visualized by using VESTA [35]. The solid line indicates the solid line unit cell, and the dashed circles indicate the possible Ca-deficient positions.

3. Results and discussions

3.1. XRD patterns and band gap of HAP and Ti-HAP

The XRD patterns of HAP and Ti-HAP powders are shown in Fig. 1. The inset in Fig. 1 shows enlarged diffraction patterns between 2θ of 35.0–39.5°. Both powders were revealed to be a single phase of an apatite structure. And in Ti-HAP, no TiO_2 phase was formed during synthesis. The arrows in the inset indicate the peak position of the monoclinic phase of HAP [22]. No monoclinic related peak appeared. Therefore, both HAP and Ti-HAP have a hexagonal structure.

Diffuse reflectance spectra of HAP, Ti-HAP and anatase-TiO_2 powders are shown in Fig. 2. The reflection edge wavelength of Ti-HAP was smaller than that of anatase-TiO_2. On the other hand, the reflection edge of HAP was out of our measurement range. In the case of anatase-TiO_2, the reflection in the VIS range was imperfect and there seemed to be small absorption in the VIS range. The measured band gap energies, which were obtained from the diffuse reflection spectra, are listed in Table 1. Since the measured band gap energy of TiO_2, 3.27 eV, was similar to a generally known value of 3.2 eV [35], this measurement seems to be reliable. The measured band gap energy of HAP was greater than 6 eV. This means that the band gap of HAP exceeds the measuring limit of the equipment. Since the DFT-calculated band gaps of HAP reported in references

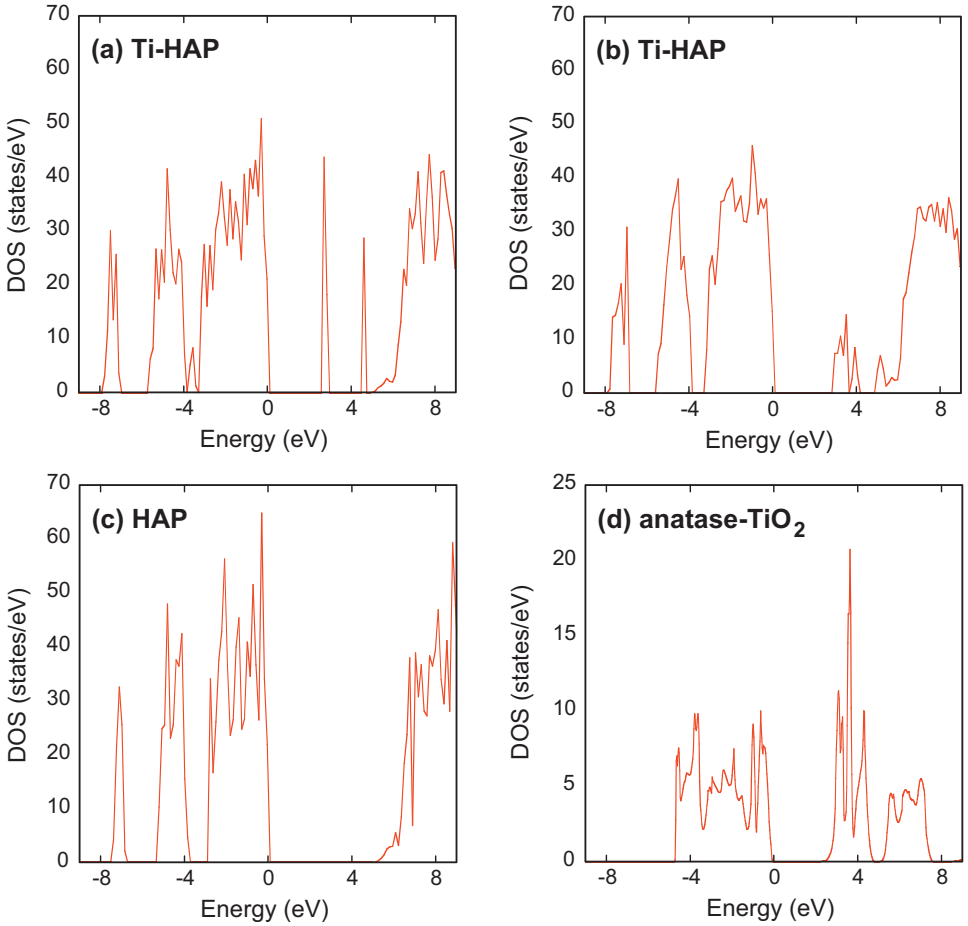

Fig. 4. Density of states: (a) Ti-HAP [Model-3], (b) Ti-HAP [Model-6], (c) HAP, and (d) anatase-TiO_2. 0 eV indicate the Fermi level.

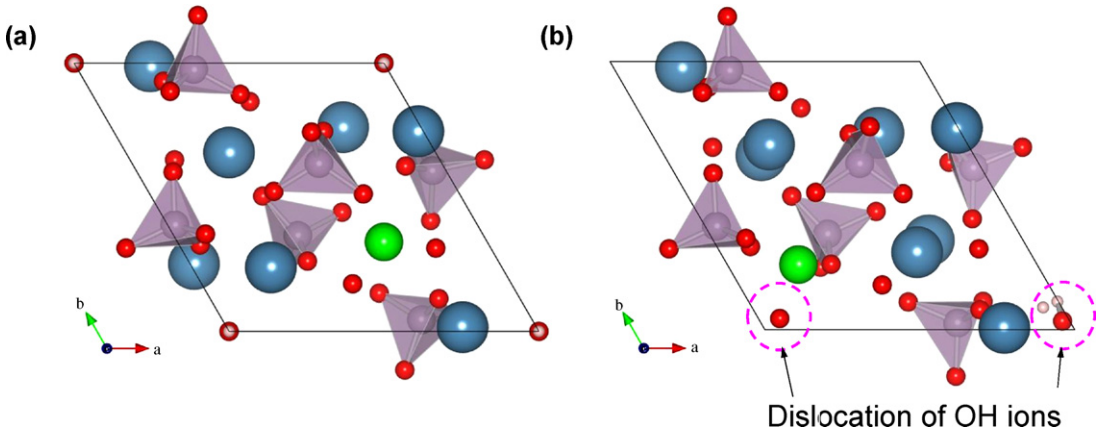

Fig. 5. Optimized unit cell structure of Ti-HAP visualized by VESTA [35]: (a) Model-3, (b) Model-6.

Table 1
Band gap energy of HAP, Ti-HAP and anatase-TiO_2 measured by diffuse reflectance spectroscopy.

Materials	Band gap energy (eV)
HAP	>6
Ti-HAP	3.65
Anatase-TiO_2	3.27

were around 4.51–5.4 eV as mentioned above, our measured band gap is quite reasonable, considering the underestimation of the band gap energy produced with the DFT calculation. The measured band gap energy of Ti-HAP was 3.65 eV. This is larger than that of TiO_2; however, it appears that Ti-HAP exhibits photocatalytic activity in the near-ultraviolet region. It was reported in Ref. [10] that the photocatalytic activity of Ti-HAP was lower than TiO_2, and the results of this study seem to confirm the contents of Ref. [10].

3.2. Calculated band gap and density of states

At first, we started calculation of Ti-HAP depending on the chemical formula of $Ca_9Ti(PO_4)_6(OH)_2$ defined in Ref. [10]. However, it may be impossible to maintain the charge neutrality by only substituting Ca^{2+} with Ti^{4+}. Accordingly, there was a possibility of a Ca deficiency existing at the nearest neighboring position of the Ti atom. We therefore defined the chemical formula of Ti-HAP as $Ca_8Ti(PO_4)_6(OH)_2$. Moreover, it was difficult to determine the Ti position simply, because the Ca ion can easily be exchanged with various cations [7–9]. Zhu et al. evaluated the occupation of the metal ion in HAP and concluded that ions with a larger radius and larger electronegativity than the Ca ion seemed to occupy the Ca(II) site [36]. Ti has a larger electronegativity than Ca. However, its ionic radius is smaller. Therefore, it seems possible that Ti can occupy both the Ca(I) and Ca(II) site. Six Ti-HAP structure models were then premised as shown in Fig. 3 visualized with VESTA software [37]. Fig. 3(a) shows Ti-substituted Ca(I) site, and three capable Ca deficient positions are indicated with the dashed circles from Model-1 to -3. In Fig. 3(b), the Ti-substituted Ca(II) site and Ca deficient are indicated as Model-4 to -6 in the same manner in Fig. 3(a).

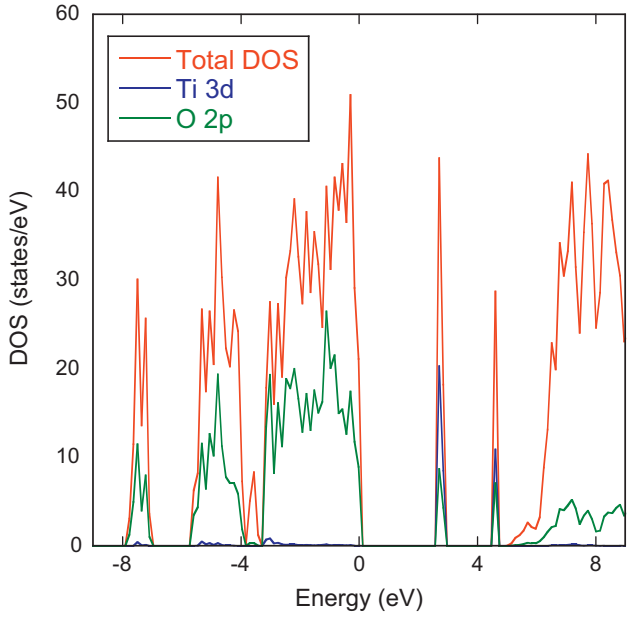

Fig. 6. Total and projector DOS of Ti-HAP [Model-3]; 0 eV indicate the Fermi level.

Table 2
Calculated total energy and band gap energy of estimated Ti-HAP structures.

Structure	Ti position	Ca deficient	Total energy (Ry)	Band gap (eV)
Model-1	Ca(I)	Ca(II)	−697.3991	1.94
Model-2	Ca(I)	Ca(II)	−697.4000	1.82
Model-3	Ca(I)	Ca(I)	−697.4065	2.74
Model-4	Ca(II)	Ca(I)	−697.3809	1.94
Model-5	Ca(II)	Ca(II)	−697.3918	1.80
Model-6	Ca(II)	Ca(II)	−697.4252	2.95

The total energy and band gap energy in the six premised structures are listed with the Ti and Ca-deficient position in Table 2. Among the structures in which Ti was substituted in the Ca(I) site, Model-3 shows the lowest total energy and seems to be the most stable. With the Ca(II)-substituted structure, Model-6 seems to be the most stable. Therefore these two models seem to be possible Ti-HAP structures. The above-mentioned two structures have band gap energies of 2.74 and 2.95 eV, respectively. The calculated band gap of anatase-TiO_2 was 2.23 eV, which was similar to the value shown in Refs. [38–40]. The band gap of Model-3 and Model-6 is larger than that of the theoretically calculated anatase-TiO_2. This relative tendency of variation is similar with the experimental results shown in Table 1. The DOS of the Model-3 and Model-6 structures of Ti-HAP are shown in Fig. 4(a) and (b) compared with HAP and anatase-TiO_2 [Fig. 4(c) and (d)]. Although the band gap energy of HAP was 4.95 eV in Fig. 4(c), new states were formed in between the valence band and the conduction band when Ti were substituted into HAP as shown in Fig. 4(a) and (b) of Ti-HAP. These states decreased the band gap energy and seemed to contribute to the absorption edge increasing to near UV range.

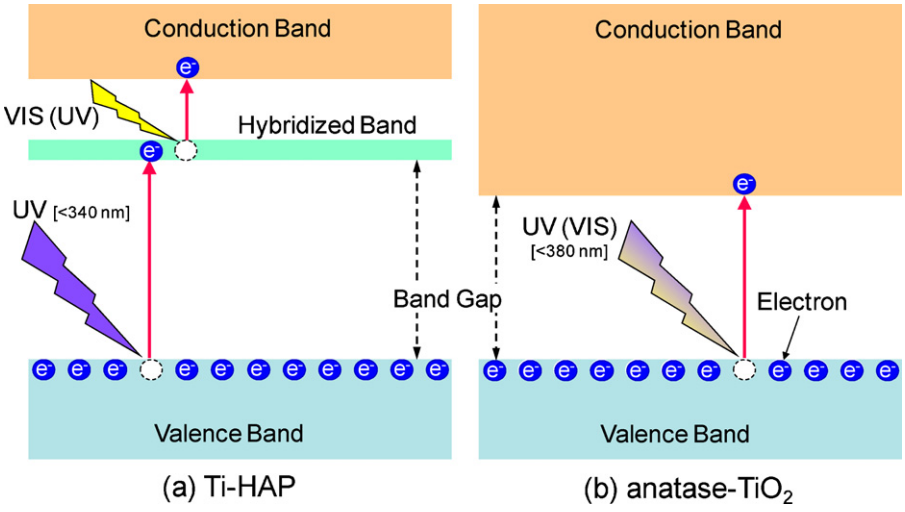

Fig. 7. Schematic photocatalytic model of (a) Ti-HAP and (b) anatase-TiO_2.

The optimized unit cell structures of Ti-HAP, Model-3, and Model-6, are shown in Fig. 5. In Model-6, two OH ions were dislocated and formed one H_2O molecule and one oxygen atom. It is possible for crystallohydrate to exist on the surface of Ti-HAP. However, when considering the heat treatment at 650 °C, it does not seem to be a real hydroxyapatite-based structure, which has H_2O molecule in all unit cells after heat treatment. Therefore, Model-3 seems to be the most appropriate structure of photocatalytic Ti-HAP.

Fig. 6 shows the total and projector DOS of O 2p and Ti 3d orbital of Model-3. The DOS of O 2p indicates the sum of DOS from the nine nearest neighboring O atoms around the Ti atom. Ti 3d and O 2p form a hybrid orbital. However, since these states were very narrow, the hybrid orbital was caused by weak covalent bonding of the Ti atom and O atoms. Such hybrid orbital seems to reduce the band gap energy and photo-absorption edge of Ti-HAP compared with HAP. However, the hybrid orbital does not exist in the conduction band. Therefore, photocatalytic activity may not occur only with single photon absorption.

Following on from the above discussion, in Ti-HAP, a scenario of photo-induced excitation is considered as follows: the electron in the valence band can be excited to hybridized states by absorption of the near UV photon and then subsequently excited to the conduction band by absorption of an additional photon. The schematic model of this scenario is shown in Fig. 7 with the anatase-TiO_2 model. In consideration of Fig. 7(a), we anticipated that it would be possible for the second excitation to occur with the absorption of the VIS photon.

3.3. *Photocatalytic activity for acetaldehyde gas decomposition by UV and VIS*

To confirm the above discussed photocatalytic model and expectation of Ti-HAP, we evaluated acetaldehyde gas decomposition with UV and VIS light. The results are shown in Fig. 8. CO_2 concentration resulting from acetaldehyde gas decomposition of Ti-AHP was smaller than that of anatase-TiO_2. This is because, as shown in Table 1, the band gap of Ti-HAP is larger than that of anatase-TiO_2. Moreover, the band gap of Ti-HAP exceeded the range of VIS. Therefore, almost no decomposition had occurred through irradiation of VIS in Fig. 8(a). However, both UV and VIS were irradiated simultaneously on Ti-HAP, and the CO_2 concentration resulting from the gas decomposition increased and exceeded that when UV irradiation alone was applied.

As Fig. 8(b) indicates, anatase-TiO_2 also shows additional gas decomposition by UV + VIS irradiation compared with UV irradia-

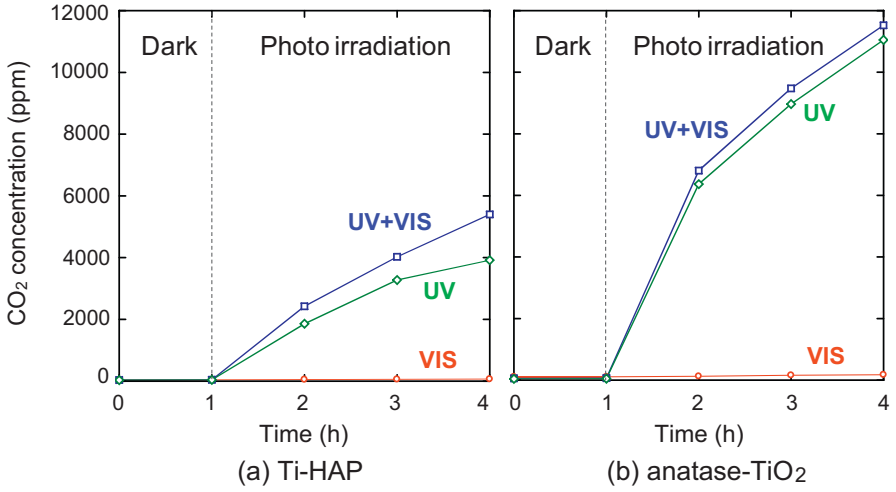

Fig. 8. Photocatalytic activity of (a) Ti-HAP and (b) anatase-TiO_2 powder; decomposition of acetaldehyde to CO_2 by photo irradiation. Band pass filters: UV cut (≤420 nm), VIS cut (≥400 nm), Quantity of light: UV: 1.25 mW/cm^2, VIS: 36,200 lux.

tion alone. The anatase-TiO_2, evaluated in this study, showed an increase in the CO_2 concentration through irradiation of VIS. It seems that, as shown in Fig. 2, reflection of anatase-TiO_2 in the VIS area was smaller than that of Ti-HAP and HAP. Then, it may be possible for small acetaldehyde gas decomposition to occur through VIS irradiation to anatase-TiO_2. Therefore, the photocatalytic phenomenon of Ti-HAP by UV + VIS irradiation seems to be different from that of anatase-TiO_2.

Depending on the above results and discussion, our estimated atomic structure and photocatalytic model of Ti-HAP seems to be confirmed. However, in this study, the adapted atomic structure of Ti-HAP was premised only with DFT calculations, and so it is important to determine the Ti position in Ti-HAP experimentally. Experimental efforts to identify Ti positions are being conducted using the neutron diffraction technique and X-ray absorption fine structure (XAFS) analysis.

4. Conclusions

In summary, we evaluated the band gap of Ti-HAP experimentally and theoretically in comparison with anatase-TiO_2. The experimental band gaps of HAP, Ti-HAP, and anatase-TiO_2 were greater than 6 eV, 3.65 eV, and 3.27 eV, respectively. The DFT-calculated band gaps of HAP, Ti-HAP, and anatase-TiO_2 were 4.95 eV, 2.74 eV, and 2.23 eV, respectively. By comparing optimized unit cell structures, in Ti-HAP, Ti seems to substitute the Ca(I) site with the Ca(I) site deficient. In Ti-HAP, Ti 3d orbital hybridized with the O 2p orbital and formed a lower state in the HAP band gap. It caused the absorption-edge lowering of Ti-HAP. The photocatalytic activity of Ti-HAP was enhanced with UV + VIS irradiation compared with only UV irradiation.

Acknowledgments

The authors would like to thank Professor Isao Tanaka and Associate Professor Katsuyuki Matsunaga of Kyoto University for their valuable suggestions.

References

[1] J.C. Elliott, Structure and Chemistry of the Apatite and Other Calcium Orthophosphates, Elsevier, Amsterdam, 1994.
[2] R.Z. LeGeros, in: P.W. Brown, B. Constanz (Eds.), Hydroxyapatites and Related Materials, CRC Press, London, 1994.
[3] J.A.S. Bett, L.G. Christner, W.K. Hall, J. Am. Chem. Soc. 89 (1967) 5535–5540.
[4] S. Sugiyama, T. Minami, T. Moriga, H. Hayashi, K. Koto, M. Tanaka, J.B. Moffat, J. Mater. Chem. 6 (1996) 459.
[5] Y. Matsumura, H. Kanai, J.B. Moffat, J. Chem. Soc. Faraday Trans. 93 (1997) 4383–4389.
[6] F. Monroe, W. Votava, D.B. Bass, J. McMullen, J. Dent. Res. 50 (1971) 860–861.
[7] T. Suzuki, T. Hatsushika, Y. Hayakawa, J. Chem. Soc., Faraday Trans. 77 (1981) 1059–1062.
[8] T. Suzuki, T. Hatsushika, M. Miyake, J. Chem. Soc., Faraday Trans. 77 (1982) 3605–3611.
[9] H. Monma, Shokubai 27 (1985) 237–243 [in Japanese].
[10] M. Wakamura, K. Hashimoto, T. Watanabe, Langmuir 19 (2003) 3428–3431.
[11] H. Nisikawa, Mater. Lett. 58 (2003) 14–16.
[12] H. Nisikawa, K. Omamiuda, J. Mol. Catal. A Chem. 179 (2002) 193–200.
[13] H. Nisikawa, J. Mol. Catal. A Chem. 206 (2003) 331–338.
[14] H. Nisikawa, J. Mol. Catal. A Chem. 207 (2004) 149–153.
[15] H. Nishikawa, Phos. Res. Bull. 17 (2004) 101–104.
[16] H. Nishikawa, Phos. Res. Bull. 21 (2007) 97–102.
[17] C.C. Ribeiro, I. Gibson, M.A. Barbosa, Biomaterials 27 (2006) 1749–1761.
[18] H. Anmin, L. Ming, C. Chengkang, M. Dali, J. Mol. Catal. A Chem. 267 (2007) 79–85.
[19] C. Hu, J. Guo, J. Qu, X. Hu, Appl. Catal. B Environ. 73 (2007) 345–353.
[20] C. Ergum, J. Eur. Ceram. Soc. 28 (2008) 2137–2149.
[21] G. Rosenman, D. Aronov, L. Oster, J. Haddad, G. Mezinskis, I. Pavlovska, M. Chaikina, A. Karlov, J. Lumin. 122–123 (2007) 936–938.
[22] D. Haverty, S.A.M. Tofail, K.T. Stanton, J.B. McMonagle, Phys. Rev. B 71 (2005) 094103-1–094103-9.
[23] L. Calderin, M.J. Stott, A. Rubio, Phys. Rev. B 67 (2003) 134106-1–134106-7.
[24] P. Rulis, L. Ouyang, W.Y. Ching, Phys. Rev. B 70 (2004) 155104-1–155104-8.
[25] K. Matsunaga, A. Kuwabara, Phys. Rev. B 75 (2007) 014102-1–014102-9.
[26] D.U. Schramm, J. Terra, A.M. Rossi, D.E. Ellis, Phys. Rev. B 63 (2000) 024107-1–024107-14.
[27] M. Jiang, J. Terra, A.M. Rossi, M.A. Morales, E.M. Baggio Saitovitch, D.E. Ellis, Phys. Rev. B 66 (2002) 224107-1–224107-15.
[28] R. Astala, M.J. Stott, Chem. Mater. 17 (2005) 4125–4133.
[29] R. Astala, L. Calderín, X. Yin, M.J. Stott, Chem. Mater. 18 (2006) 413–422.
[30] X. Ma, D.E. Ellis, Biomaterials 29 (2008) 257–265.
[31] K. Matsunaga, J. Chem. Phys. 128 (2008) 245101-1–245101-10.
[32] K. Matsunaga, H. Inamori, H. Murata, Phys. Rev. B 78 (2007) 094101-1–094101-8.
[33] The original "PHASE" code is developed in the Frontier Simulation Software for Industrial Science project (FSIS) and commercialized as "Advance/PHASE" by AdvanceSoft Corporation. http://www.ciss.iis.u-tokyo.ac.jp/fsis/en/index.html, http://www.advancesoft.jp/product/advance_phase.
[34] J.P. Perdew, K. Burke, M. Ernzerhof, Phys. Rev. Lett. 77 (1996) 3865–3868.
[35] L. Kavan, M. Grätzel, S.E. Gilbert, C. Klemenz, H.J. Scheel, J. Am. Chem. Soc. 118 (1996) 6716–6723.
[36] K. Zhu, K. Yanagisawa, R. Shimanouchi, A. Onda, K. Kajiyoshi, J. Euro. Ceram. Soc. 26 (2006) 509–513.
[37] K. Monma, F. Izumi, J. Appl. Crystallogr. 41 (2008) 653–658.
[38] W. Li, Y. Wang, H. Lin, S. Ismat Shah, C.P. Huang, D.J. Doren, S.A. Rykov, J.G. Chen, M.A. Barteau, Appl. Phys. Lett. 83 (2003) 4143–4145.
[39] H. Kamisaka, T. Adachi, K. Yamashita, J. Chem. Phys. 123 (2005) 084704-1–084704-9.
[40] M. Long, W. Cai, Z. Wang, G. Liu, Chem. Phys. Lett. 420 (2006) 71.